NRC·CNRC

NRC Publications Archive
Archives des publications du CNRC

Behavior of the residual wave components in a 3D wave basin after the termination of the wave maker

Zaman, M. Hasanat; Mak, Lawrence; Millan, Jim; Kuczora, Andrew

This publication could be one of several versions: author's original, accepted manuscript or the publisher's version. / La version de cette publication peut être l'une des suivantes : la version prépublication de l'auteur, la version acceptée du manuscrit ou la version de l'éditeur.
For the publisher's version, please access the DOI link below./ Pour consulter la version de l'éditeur, utilisez le lien DOI ci-dessous.

Publisher's version / Version de l'éditeur:
https://doi.org/10.1115/OMAE2015-41850
ASME 2015 34th International Conference on Ocean, Offshore and Arctic Engineering: May 31-June 5, 2015, St. John's, Newfoundland, Canada, 7, 2015-06

NRC Publications Record / Notice d'Archives des publications de CNRC:
https://nrc-publications.canada.ca/eng/view/object/?id=8f7449bf-b80b-4567-a5b1-ab5f61239974
https://publications-cnrc.canada.ca/fra/voir/objet/?id=8f7449bf-b80b-4567-a5b1-ab5f61239974

Access and use of this website and the material on it are subject to the Terms and Conditions set forth at https://nrc-publications.canada.ca/eng/copyright
READ THESE TERMS AND CONDITIONS CAREFULLY BEFORE USING THIS WEBSITE.

L'accès à ce site Web et l'utilisation de son contenu sont assujettis aux conditions présentées dans le site https://publications-cnrc.canada.ca/fra/droits
LISEZ CES CONDITIONS ATTENTIVEMENT AVANT D'UTILISER CE SITE WEB.

Questions? Contact the NRC Publications Archive team at PublicationsArchive-ArchivesPublications@nrc-cnrc.gc.ca. If you wish to email the authors directly, please see the first page of the publication for their contact information.

Vous avez des questions? Nous pouvons vous aider. Pour communiquer directement avec un auteur, consultez la première page de la revue dans laquelle son article a été publié afin de trouver ses coordonnées. Si vous n'arrivez pas à les repérer, communiquez avec nous à PublicationsArchive-ArchivesPublications@nrc-cnrc.gc.ca.

National Research Council Canada | Conseil national de recherches Canada

Canada

Proceedings of the ASME 2015 34th International Conference on Ocean, Offshore and Arctic Engineering
OMAE2015
May 31 - June 5, 2015, St. John's, Newfoundland, Canada

OMAE2015-41850

BEHAVIOR OF THE RESIDUAL WAVE COMPONENTS IN A 3D WAVE BASIN AFTER THE TERMINATION OF THE WAVE MAKER

M Hasanat Zaman
National Research Council Canada
Ocean, Coastal and River Engineering
Arctic Ave., PO Box 12093, Station A
St. John's, NL, A1B 3T5, Canada

Lawrence Mak
National Research Council Canada
Ocean, Coastal and River Engineering
Arctic Ave., PO Box 12093, Station A
St. John's, NL, A1B 3T5, Canada

Jim Millan
National Research Council Canada
Ocean, Coastal and River Engineering
Arctic Ave., PO Box 12093, Station A
St. John's, NL, A1B 3T5, Canada

Andrew Kuczora
National Research Council Canada
Ocean, Coastal and River Engineering
Arctic Ave., PO Box 12093, Station A
St. John's, NL, A1B 3T5, Canada

ABSTRACT

After the termination of the wave making, the characteristics of the existing wave components in a 3D large scale Offshore Engineering wave Basin (OEB) at the National Research Council of Canada have been investigated experimentally. In the generation of any wave in the tank we get the relevant primary wave components along with bounded wave components if the incident primary wave has more than one frequency. Inevitably we also get interacted wave components, natural frequency components of the tank and other free waves. In this paper the tank's natural frequency components, bounded wave components and other free waves after the termination of wave making were investigated using several cases of mono- and bi-chromatic waves. These component energies were then compared with the total energy of the measured primary waves. The magnitudes of the residual undulations are also investigated for mono-, bi- and multi-chromatic waves over different time segments. Several sets of wave data are analysed to perceive the energy due to natural frequency of the basin, energy transferred to the side bands and the damping rate of the residual waves in the tank with respect to the chosen incident wave conditions. In the analysis it is observed that the energy damping rate varies with the incident wave condition but seems much faster than that of 20 minutes traditional waiting time in between two runs in the OEB. The energies for tank's natural frequency components and other free waves were found to be very small compare to the incident primary wave energies.

KEYWORD

Physical experiments, *mono-, bi- and multi-chromatic waves, energy damping*, *natural energy components of the tank, residual undulation over time*, *data comparisons*.

INTRODUCTION

When waves are generated in the basin the available frequencies interact among themselves in various forms and the wave energies are transferred to the interacted frequency bands. It is very crucial to generate correct waves in the wave tanks for any model test as this data would be used to design prototype structures in the real ocean. The reliability of the ocean structures will largely depend on the design parameters that can be obtained from an accurate experimental work. So it is very imperative to account for the magnitude of all the wave components in the wave tank when a new wave is about to be generated. We need to understand the characteristics and magnitude of the residual surface undulations in the tank over time after the wave making is terminated. This information will help the wave tank (OEB) users to reduce or increase the waiting-time as required in between consecutive "runs" to ensure consistent data quality. The model test results would be

 Copyright © 2015 by National Research Council Canada

jeopardized due to the presence of the relatively large amplitude residual surface undulations. So we have to be sure that the available surface undulation is already small enough not to contaminate the next "run". When we generate waves in the tank we obtain the primary wave components, bounded waves, interacted wave components, unwanted free wave components [Zaman et al. (2010 and 2011), Zaman and Mak (2007), Mansard et al.(1987), Sand and Mansard (1986)] and some contribution of natural frequency energy components of the wave tank. Interactions of the wave components are numerous but are not necessarily important due to their small amplitudes. Low frequency bounded waves are obtained from frequency differences. Tank natural frequency energy components are obtained from the data measured after the wave making was stopped. We measured data for 20 minutes (min) where wave making was ended after first 3min. The reason is to observe the residual surface undulations in different time segments over the last 17min of the record and also to identify the natural frequency energy components of the tank. Several mono- and bi-chromatic waves were tested over three different water depths (0.4*m*, 0.5*m* and 0.6*m*) in this experiment.

Results are compared for different wave components of both mono- and bi-chromatic waves. The natural frequency energy components along the longitudinal and transverse directions of the tank are compared with the primary wave components and discussed in this paper. It is also found that the natural frequency components for both longitudinal and transverse directions of the tank were very small compare to the primary wave components at least in the cases that we considered here.

For multi-chromatic waves a water depth of 2.28m was used. Two sets of multi-chromatic wave data are analyzed to perceive the rate of damping when wave making was stopped.

The primary aim of this paper is to report the damping behaviour of the OEB in the presence of different incident waves shown in Tables 3 to 5. The damping scenario might be different in the presence of structures either free-floating or moored in the OEB. In the next phase a robust procedure would be developed to identify the damping condition using real time data from a dedicated wave probe in the tank and also from a qualisys system with 3 degrees translation and 3 degrees of rotational motions.

NATURAL FREQUENCY IN A BASIN

The OEB is a rectangular basin with significant length (= 72*m*), width (= 26*m*) and depth (= 3*m*). The natural periods and frequencies can be estimated using the following equations (Mei, 1999):

$$T_{nm} = \frac{2}{\sqrt{gh}}\left[\left(\frac{n}{a}\right)^2 + \left(\frac{m}{b}\right)^2\right]^{-\frac{1}{2}}; \qquad c = \sqrt{gh} \tag{1}$$

$$f_{nm} = \frac{1}{T_{nm}} \quad ; \quad n, m = 0, 1, 2, ... \tag{2}$$

where T_{nm} and f_{nm} are natural period and frequency, h (= 3*m*) is the depth, a (= 72*m*) is the length and b (= 26*m*) is the width of the basin.

Table 1 Computed natural period of the tank

Transverse components				
Modes	n	m	Computations of T_{nm}	T_{nm}
Ist	0	1	$T_{01} = \frac{1}{f_{01}} = \frac{2}{\sqrt{gh}}.b$	9.578
2nd	0	2	$T_{02} = \frac{1}{f_{02}} = \frac{2}{\sqrt{gh}}.\frac{b}{2}$	4.789
3rd	0	3	$T_{03} = \frac{1}{f_{03}} = \frac{2}{\sqrt{gh}}.\frac{b}{3}3$	3.192
Longitudinal components				
Ist	1	0	$T_{10} = \frac{1}{f_{10}} = \frac{2}{\sqrt{gh}}.a$	26.524
2nd	2	0	$T_{20} = \frac{1}{f_{20}} = \frac{2}{\sqrt{gh}}.\frac{a}{2}$	13.262
3rd	3	0	$T_{30} = \frac{1}{f_{30}} = \frac{2}{\sqrt{gh}}.\frac{a}{3}$	8.841

Equations 1 and 2 are used to compute the transverse and longitudinal mode components shown in Table 1:

DESCRIPTION OF THE EXPERIMENTAL SETUP

The experiment was carried out at the Offshore Engineering Basin of National Research Council Canada, St. John's. The top view of the basin is shown in Fig. 1. The Offshore Engineering Basin is 75 m long and 32 m wide. Fifty two (52) independently controlled segmented wave generators installed on the west wall generated the waves. Each segmented wave generator is 2 m high and 0.5 m wide.

Table 2 Location of the wave probes in the OEB

No of the probe	Distance from the east wave paddle (m)	Distance from the south wall (m)
1	26.891	13.475
2	27.221	13.475
3	27.731	13.475
4	27.731	12.955
5	27.731	12.635
6	27.731	14.825
7	27.731	18.365
8	29.081	13.475
9	32.621	13.475
10	41.621	13.475
11	2.0	12.635
12	2.0	13.475
13	2.0	18.365
14	10.744	13.475

Passive absorbers, made of expanded metal sheets with varying porosities and spacing are installed on the east wall. A

 Copyright © 2015 by National Research Council Canada

solid metal wall was used to cover the north side of the basin. The water depths for the experiments were 0.4m, 0.5m and 0.6m. During the experiment, 14 wave probes were installed as shown in Fig. 1. Table 2 shows the locations of the wave probes throughout the basin. All the wave probes were capacitance type. All the data was acquired using GDAC (GEDAP Data Acquisition and Control) client-server acquisition system, developed by National Research Council Canada.

For multi-chromatic wave cases, five wave probes were deployed at different locations in the basin continuously for 9 (nine) months for data acquisition. Numerous data are collected during this time for different water depths (up to 2.8m water depth), incident wave heights and periods and, also in the presence or in the absence of physical models in the OEB. The rates of energy damping for multi-chromatic wave cases are only shown in this paper.

EXPERIMENTAL CONDITIONS

In the experiments both mono- and bi-chromatic waves of varying wave periods, wave heights and water depths were used. Table 3 shows some incident wave conditions for mono-chromatic waves that we used in this experiment where T is the wave period, H the wave heights, h the still water depth and h/L is the relative water depth that identifies the wave as deep-water ($h/L \geq 0.5$) or shallow-water wave. On the other hand, Table 4 shows several conditions for bi-chromatic incident waves where, T_1 and T_2 are the wave periods, H_1 and H_2 are the wave heights and h is the still water depth.

Table 3 Incident wave conditions for mono-chromatic waves

Cases	*h (m)*	*T (s)*	*H (m)*	*h/L*
Case-1	0.4	2.145	0.08	0.10
Case-2	0.4	4.105	0.08	0.05
Case-3	0.5	1.977	0.08	0.125

The bottom of the basin was flat and the blanking plates were deployed to cover the north beach.

Table 4 Incident wave conditions for bi-chromatic wave

Cases	*h (m)*	T_1 *(s)*	T_2 *(s)*	H_1, H_2 *(m)*	$h/L_{2,22}$
Case-4	0.4	2.22	2.0	0.06	0.096
Case-5	0.5	2.22	2.0	0.06	0.109
Case-6	0.6	2.22	2.0	0.06	0.121

Table 5 shows the multi-chromatic waves that we used in the experiment where H_s is the significant wave height and T_p is the peak wave period.

Table 5 Incident wave conditions for multi-chromatic wave

Cases	*h (m)*	T_p *(s)*	H_s *(m)*	h/L_{Tp}
Case-7	2.28	1.3	0.07	0.864
Case-8	2.28	2.6	0.39	0.238

METHODOLOGY, SCOPE AND LIMITATIONS

This paper reports the first phase of the project to identify and quantify the natural frequency components in the OEB. The first phase is mostly focused on the investigation of mono-chromatic and bi-chromatic waves in details. Very limited results are also incorporated on irregular waves in this paper. Wave splitting described Mansard et al. (1987) and Zaman et al. (2010, 2011) was used to separate the different wave components – primary wave(s), bounded wave(s) and free wave(s). Natural frequency components in the longitudinal and transverse directions were identified using Equations 9 to 14. The amplitudes of the different components were estimated using spectral analysis. For typical mono- and bi-chromatic wave tests, our clients are interested in the 5-10 repeat cycles, for zero-crossing analysis, spectral analysis, response amplitude operator analysis, while minimizing wave reflection. Thus, 3 minutes is adequate time to allow for 10s ramp up, evanescent wave component, 5-10 repeat cycles and 10s ramp down. As an example we can see Case-2, the longest monochromatic wave that we have used here where T=4.105s. In 3 minutes, we have 43 cycles. Δf=0.0055Hz.

RESULTS AND DISCUSSIONS

Equations 1 and 2 were used to identify the natural periods of the tank in the longitudinal and transverse directions for different modes. As mentioned before, in this experiment the data were captured for 20min in which 17min data are after the wave making was stopped. Fig. 2 shows the normalized amplitude spectrum of the longest mono-chromatic wave that we used in this experiment, Case-2. Fig. 2 shows: (a) the amplitude spectrum of the whole 20min data, (b) the amplitude spectrum for a data slot 10-11.33min, (c) similar results at data slot 15 to 16.67min and (d) results for 18.67 to 20min data slot. These figures include the primary wave component (T), interacted wave components and tank's natural frequency components. Similar spectrum is also shown in Fig. 3 (a, b, c and d) for the bi-chromatic wave for Case-4. In this figure the components due to the interaction of the primary waves (T_1 and T_2) are also evident in addition to the other components shown in Fig. 2: (a), (b), (c) and (d). Fig. 4a shows the surface elevation data for mono-chromatic wave for Case-2 at Probe-3. Four time segments (8.0-9.33min, 10.0-11.33min, 15-15.33min and 18.67-20.0min) chosen for the analyses are shown in Fig. 4a by the vertical dashed lines. Fig. 4b shows the energy spectrum for the total 20min data set on the left y-axis along with the spectrums of the above four time segments on the right y-axis. Similarly Fig. 5a shows the total surface elevation data for Case-2 at Probe-8 and Fig. 5b shows the total and the segmental energy spectrums at the same location. Energy is computed from the area under the spectrum curves.

Fig. 6a shows the surface elevation data for bi-chromatic wave for Case-4 at Probe-1. In the bi-chromatic case three time segments (10.0-11.33m, 15-15.33m and 18.67-20.0m) were chosen shown in Fig. 6a. Fig. 6a shows the 20min surface elevation data where Fig. 6b shows the energy spectrums of the whole data and the segmental data. Similarly, Figs. 7a and 7b show surface elevation and energy spectrums at Probe-8.

 Copyright © 2015 by National Research Council Canada

Figs. 8a and 8b show the comparisons of the total energies (TE) at Probes 12-1-2-3-8 (P-12, P-1, P-2, P-3, P-8) in the longitudinal direction and at Probes 6-3-4 (P-6, P-3, P-4) in the transverse direction for mono-chromatic waves for Case-1, Case-2 and Case-3. On the other hand, Figs. 8c and 8d show the comparisons of the natural frequency energies (f_{10}, f_{20}, f_{30}) for Case-1, Case-2 and Case-3 for different nodes. For a monochromatic wave, Table 5 shows the comparisons of the total energy (TE) and natural frequency energy (NE) components (f_{10}, f_{20} and f_{30}) at probes P-1, P-2, P-3, P-4, P-6, P-8 and P-12. The comparisons [%=bounded waves energy (BE) /total energy (TE) *100 or, natural frequency energy (NE) / total energy (TE) * 100] are done with respect to the total energy at each probe location. The tables show results obtained from all 20min experimental data. P-12 was located just $2m$ away from the face of the wave maker (*see* Table 2).

Table 5 Comparisons of natural frequency with respect to total energy for Case-2 (20min data used)

Probe	TE (m^2s)	NE/TE (%)		
		f_{10}	f_{20}	f_{30}
Longitudinal probes				
P-12	7.91E-05	0.063%	0.031%	0.012%
P-1	1.01E-04	0.011%	0.019%	0.013%
P-2	1.06E-04	0.010%	0.019%	0.012%
P-3	1.04E-04	0.010%	0.019%	0.011%
P-8	1.48E-04	0.006%	0.016%	0.006%
Transverse probes				
P-4	1.02E-04	0.011%	0.021%	0.013%
P-3	1.04E-04	0.010%	0.019%	0.011%
P-6	1.02E-04	0.022%	0.028%	0.013%

Figs. 9a and 9b show the comparisons of the total energies (TE) and bounded energies (BE) at Probes 12-1-2-3-8 in the longitudinal direction and at Probes 6-3-4 in the transverse direction for bi-chromatic waves for Case-4, Case-5 and Case-6. On the other hand, Figs. 9c and 9d show the comparisons of the natural frequency energies (f_{01}, f_{10}, f_{20}, f_{30}) for Case-1, Case-2 and Case-3 for different nodes. It can be observed from Table-5 that the energies of different natural frequency components are in the range of 0.01 to 0.06% compare to the generated primary wave energy for Case-2.

For a bi-chromatic wave, Table 6 shows the percentage distribution of different energies with respect to the total energy (TE) for Case-4.

From the comparisons shown in Table-6, it is observed that bounded wave energy is just 1.0% to 2.04% compare to the primary waves of different cases considered here. On the other hand, the energies of different natural frequency components are 0.01% to 0.16% compare to the generated primary wave (Case-4) energy. In all cases it is also observed that the natural frequency energy components in the transverse direction are obtained negligible for higher modes ($f_{02} = f_{03} = ... = 0$). We did not show those values in the figures when the natural frequency components are exceptionally small.

Table 6 Comparisons of bounded wave and natural frequency with respect to total energy for Case-4 (20min data used)

Probe	TE (m^2s)	BE/TE (%)	NE/TE (%)			
			f_{01}	f_{10}	f_{20}	f_{30}
Longitudinal probes						
P-12	1.00E-04	1.069	0.017	0.024	0.011	0.056
P-1	9.31E-05	1.234	0.028	0.007	0.008	0.121
P-2	8.57E-05	1.570	0.030	0.005	0.008	0.138
P-3	8.07E-05	2.045	0.026	0.011	0.011	0.136
P-8	1.08E-04	2.413	0.018	0.008	0.011	0.090
Transverse probes						
P-4	8.72E-05	1.923	0.031	0.023	0.015	0.141
P-3	8.07E-05	2.045	0.026	0.011	0.011	0.136
P-6	7.10E-05	2.276	0.034	0.032	0.009	0.159

For multi-chromatic waves, Figs. 10 and 11 show the magnitude of the energy spectrum amplitudes for Case-7 and Case-8 at five different probe locations in the tank when the wave makings were terminated. Wave proves WP1 to WP5 were located in between probes P-8 and P-10. In the figures total 17min data after the wave maker was stopped is used. Incident wave conditions for these two cases are shown in Table 5. From the figures it is found that most of the wave energies are damped in the first the 4 to 6min slot. It is also observed that for deep water case (Case-7) the energy damping phenomenon is faster than that of the shallow water case (Case-8) as expected. The ordinates of these figures are computed by the following equation:

$$\text{Magnitude}\,(mm) = \left(\sqrt{S(\Delta f)\cdot\Delta f}\right) = \left(\sqrt{\frac{m^2}{Hz}\cdot Hz}\right)\cdot 1000 \qquad (3)$$

CONCLUSION

An extensive experimental work was carried out in the Offshore Engineering Basin of National Research Council Canada to study the relationship between the primary wave(s) and their respective unwanted free waves, basin natural frequencies and the rate of energy damping after the wave making is stopped. In this paper only three cases of mono-chromatic and three cases of bi-chromatic waves are presented and discussed but more emphasis is given to Case-2 and Case-4. In an earlier analysis it was observed that the total unwanted free wave components are in the range of 1 to 4% (Zaman et al., 2011) of the incident wave height and not discussed here. For Case-2 (mono-chromatic) it is observed that the tank's natural frequency energy components are very small compare to the total energy and is of $O(10^{-3})$ or less. On the other hand, for Case-4 these energies are also found to be in the same $O(10^{-3})$ or less. For Case-4, bounded wave energy is found to be in the range of 1 to 2.4% of the primary waves. For the cases of mono-chromatic wave (Figs. 2, 4b and 5b) the residual wave energy in the tank is found to be of $O(10^{-3})$ or less in just 5min after the wave making was stopped. Similar scenario (Figs. 3, 6b and 7b) is also observed for Case-4 after 7min. So the settling time of the tank for the cases we used is faster than it

 Copyright © 2015 by National Research Council Canada

was thought. For multi-chromatic waves it is perceived that in general most of the wave energies are damped in the first 4 to 6min after the wave making is stopped but relatively shallow water wave takes longer time for a complete dissipation.

REFERENCES

[1] Mansard, E. P. D., Sand, S. E. and Klinting, P., 1987. Sub- and super-harmonics in natural waves, *Proc. of the 6th OMAE Conf., Houston, TX, USA*.

[2] Sand, S. E. and Mansard, E. P. D., 1986. Reproduction of higher harmonic waves, *National Research Council of Canada, Hydraulic Laboratory, Technical Report* TR-HY-012.

[3] Zaman, M. H. and Mak, L., 2007. Second order wave generation technique in the laboratory, *Proc. of the 26th Int. Conf. on offshore Mech. and Arctic Eng. (OMAE-2007), ASME, San Diego, USA, 10 pages, on CD-ROM.*

[4] Zaman, M. H., Peng, H., Baddour, E., Spencer, D. and McKay, S., 2010. Identifications of spurious waves in the wave tank with shallow water, *Proc. of the 29th Int. Conf. on offshore Mech. and Arctic Eng. (OMAE-2010), ASME, Shanghai, China, 13 pages, on CD-ROM*.

[5] Zaman, M. H., Peng, H., Baddour, E. and McKay, S., 2011. Spurious waves during generation of multi-chromatic waves in the wave tank in shallow water, *Proc. of the 30th Int. Conf. on offshore Mech. and Arctic Eng. (OMAE-2011)*, The Netherlands, 9 pages, on CD-ROM.

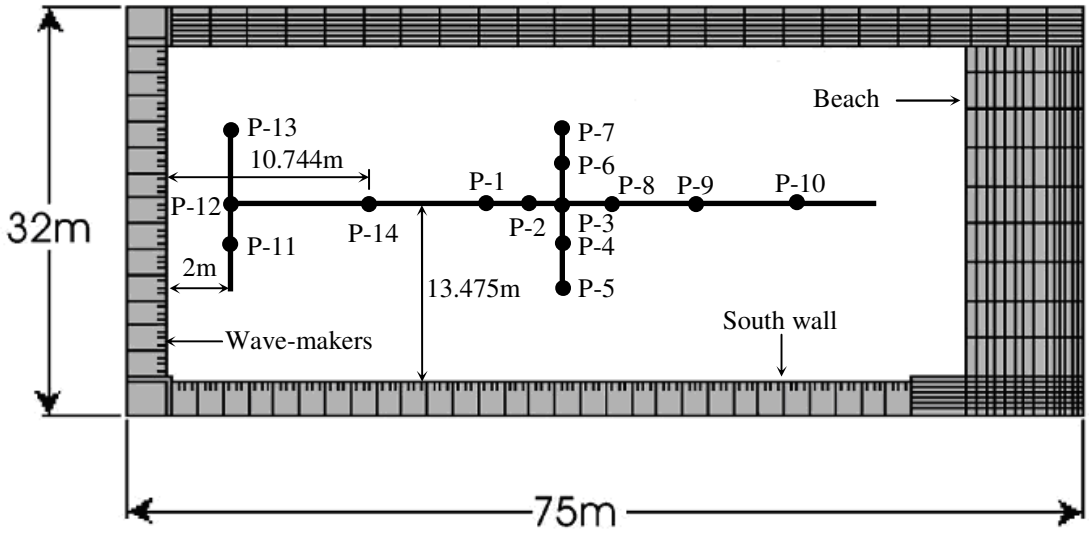

Fig. 1: Layout of the experimental tank (not to scale)

 Copyright © 2015 by National Research Council Canada

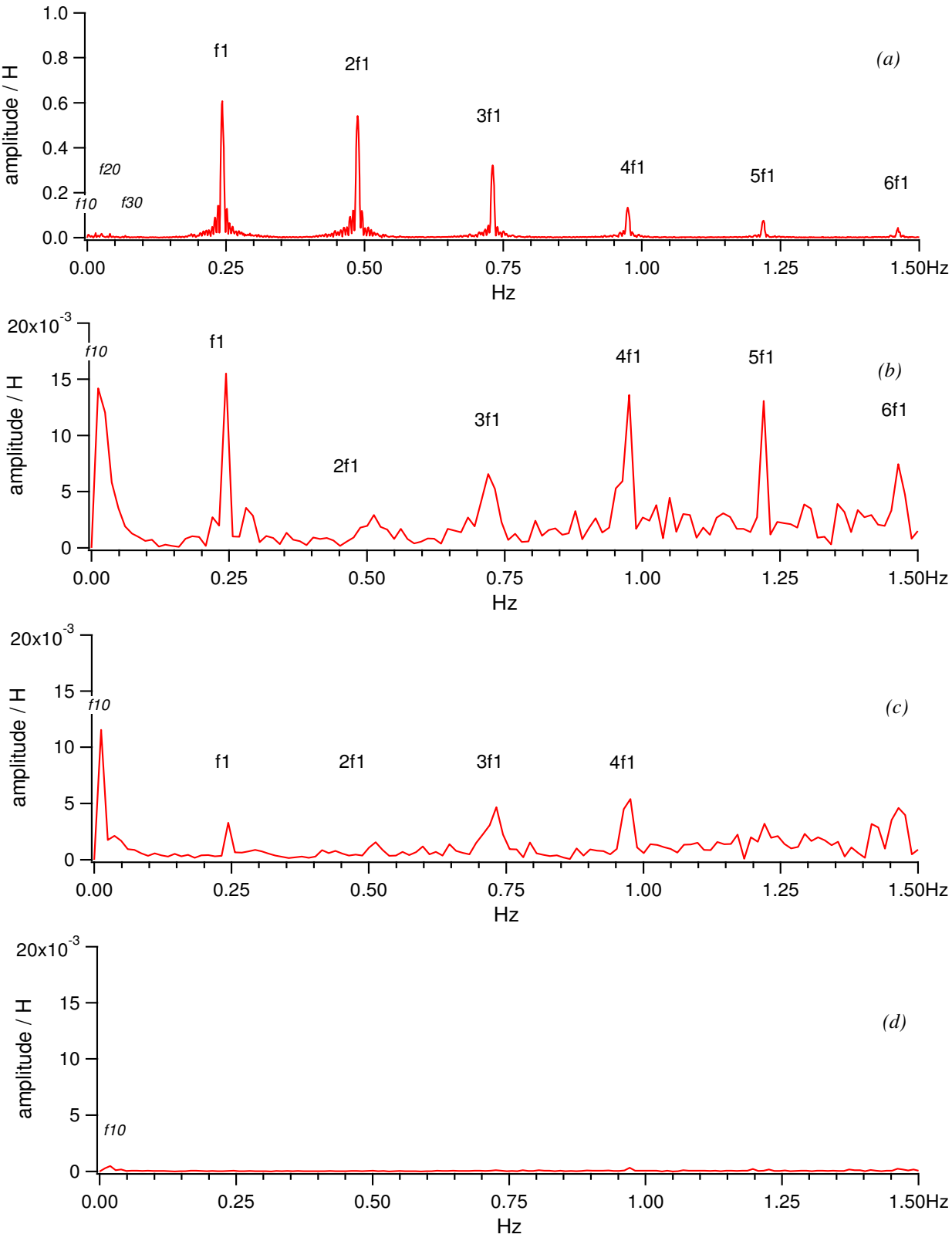

Fig. 2: Probe-3: Amplitude spectrums of: (a) Full 20min wave data (b) 10-11.33min wave data (c) 15-16.33min wave data (d) 18.67-20min wave data. Case-2: [h=0.4m, H=0.08m and T=4.105s]. Wave making was terminated after first 3min of whole 20min.

 Copyright © 2015 by National Research Council Canada

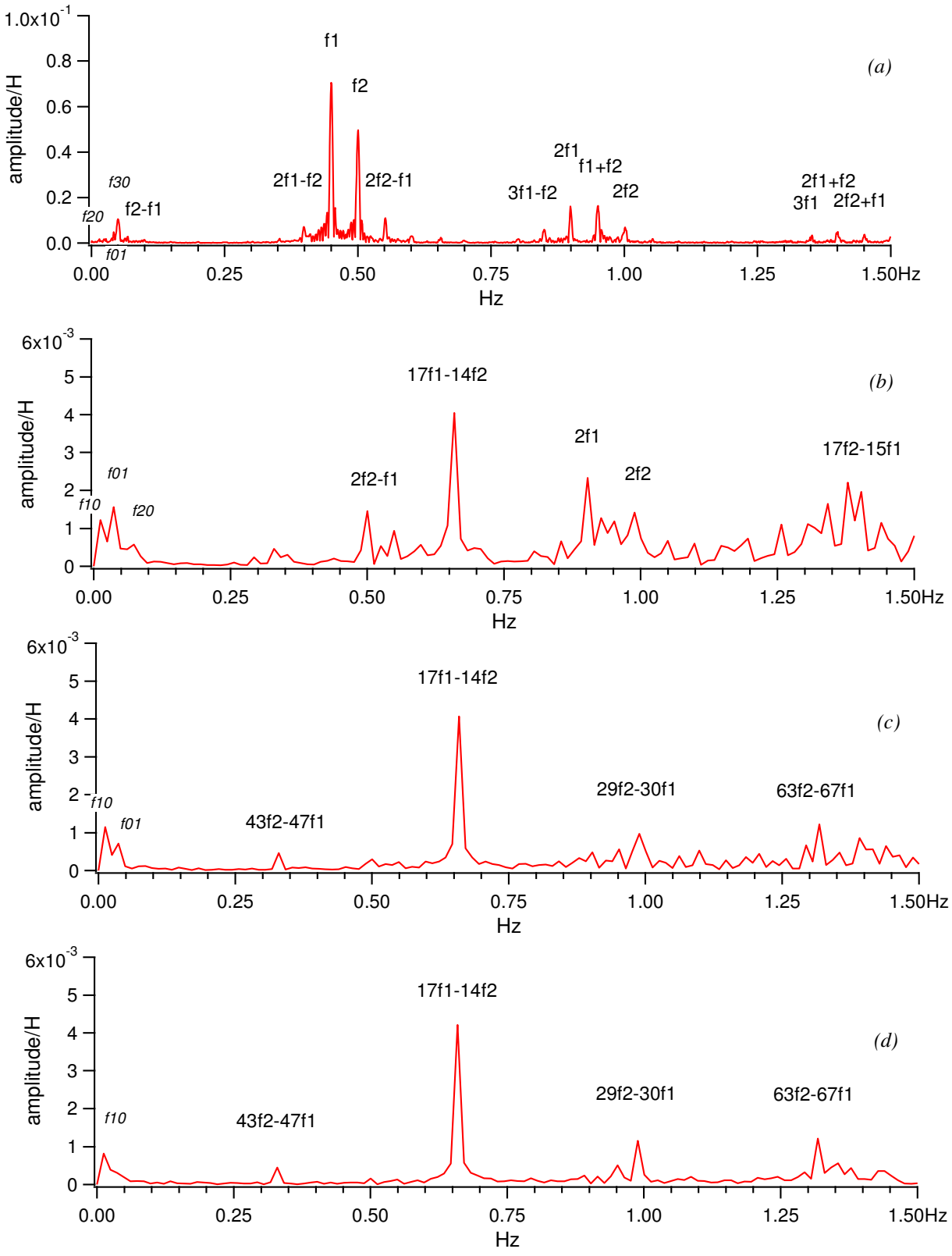

Fig. 3: Probe-1: Amplitude spectrums of: (a) Full 20min wave data (b) 10-11.33min wave data (c) in15-16.33min wave data (d) in 18.67-20min wave data. Case-4: [h=0.4m, H=0.06m, T_1=2.22s and T_2=2.0s]

 Copyright © 2015 by National Research Council Canada

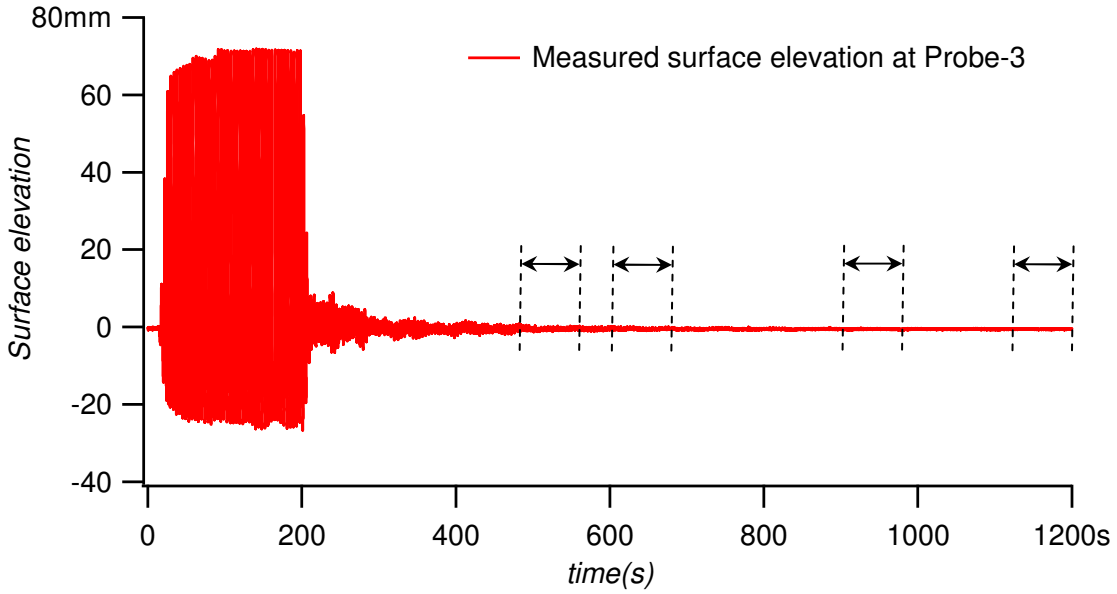

Fig. 4a Measured total surface elevation at P-1 (0 to 20min).
[h=0.4m, H=0.08m and T=4.105s]

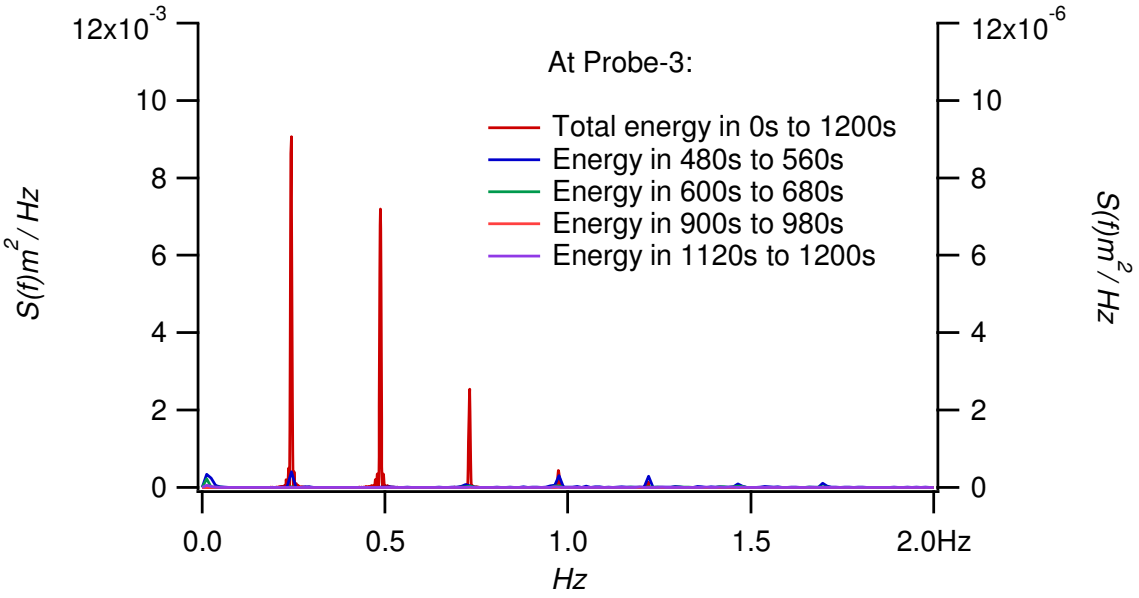

Fig. 4b Total wave energy compared with several segmental energies at P-1.
[h=0.4m, H=0.08m and T=4.105s]

 Copyright © 2015 by National Research Council Canada

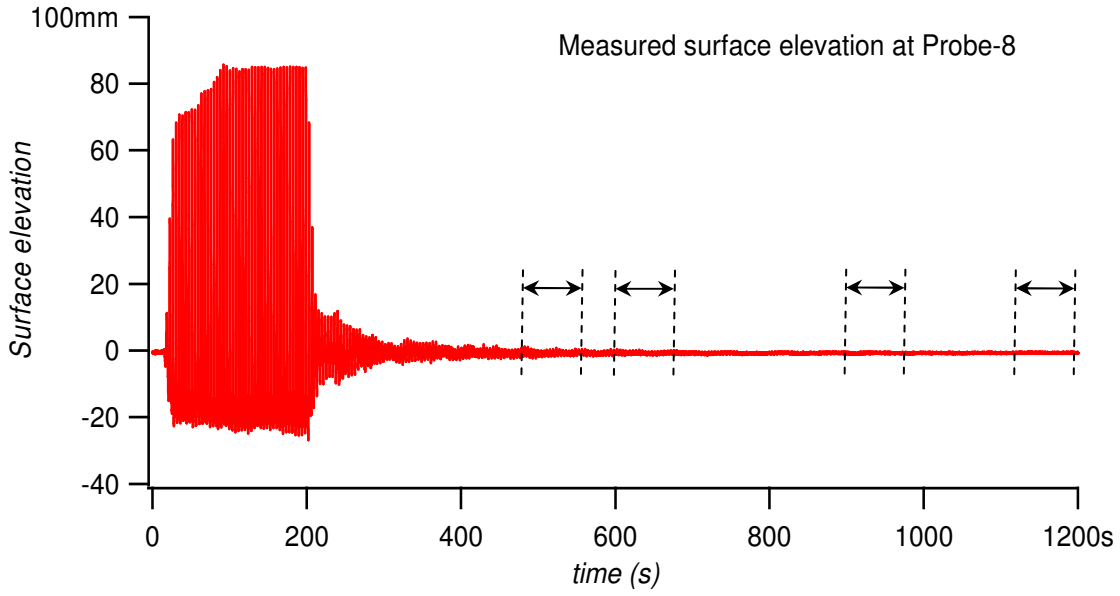

Fig. 5a Measured total surface elevation at P-8 (0 to 20min).
[h=0.4m, H=0.08m and T=4.105s]

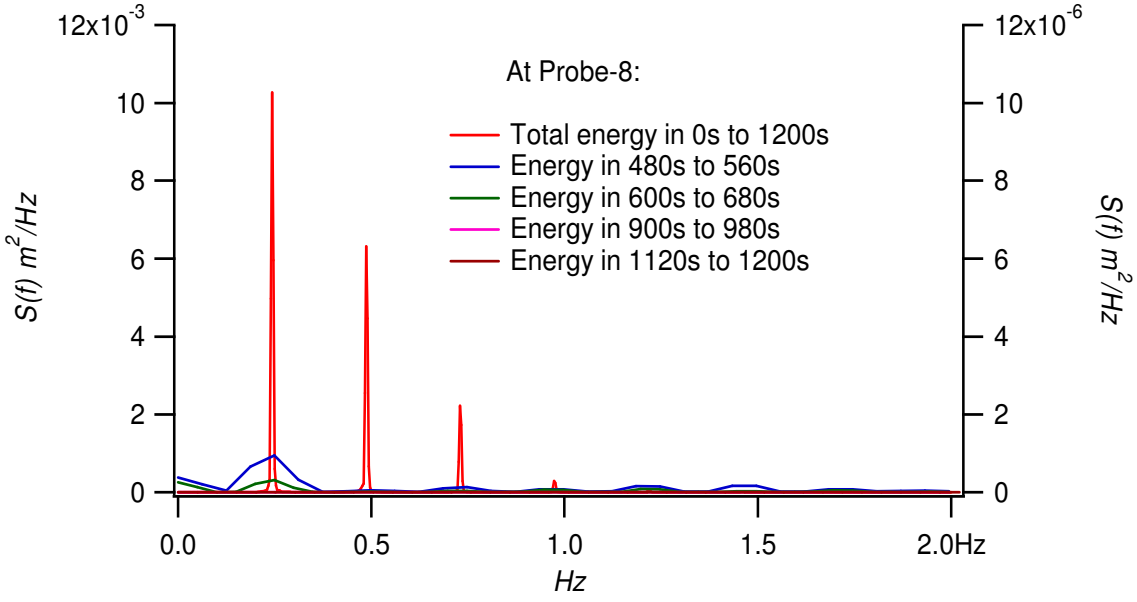

Fig. 5b Total wave energy compared with several segmental energies at P-8
[h=0.4m, H=0.08m and T=4.105s]

 Copyright © 2015 by National Research Council Canada

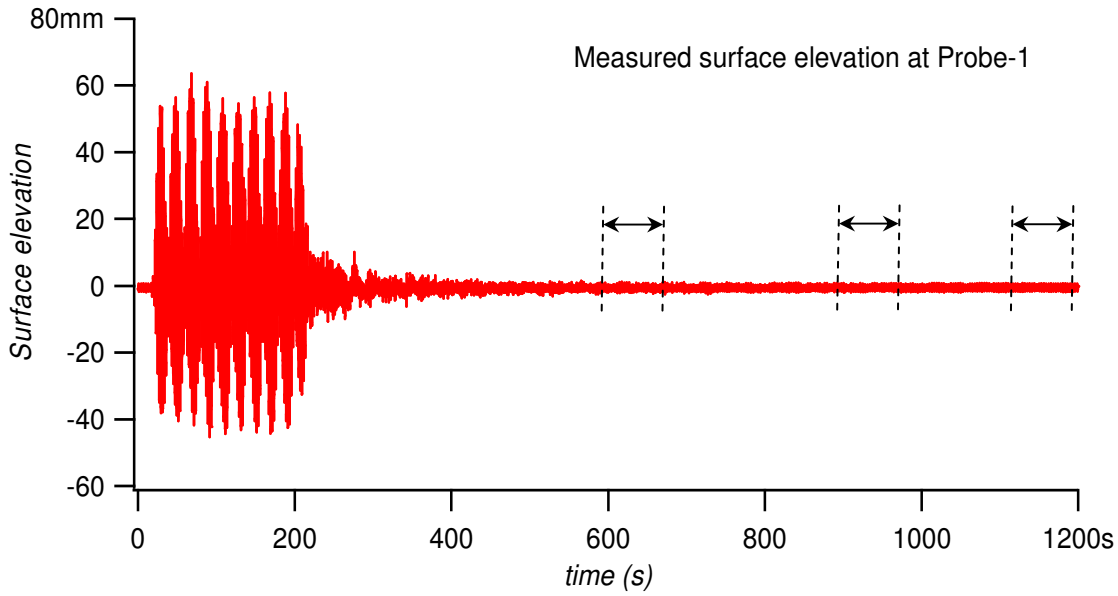

Fig. 6a Measured total surface elevation at P-1 (0 to 20min).
[h=0.4m, H=0.06m, T_1=2.22s and T_2=2.0s]

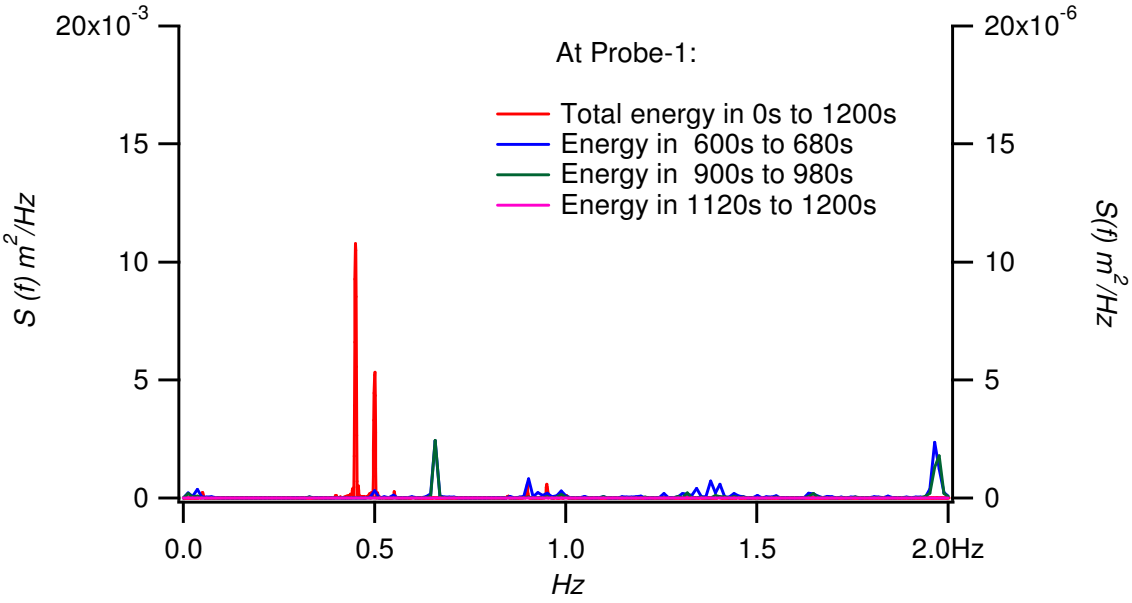

Fig. 6b Total wave energy compared with several segmental energies at P-1.
[h=0.4m, H=0.06m, T_1=2.22s and T_2=2.0s]

 Copyright © 2015 by National Research Council Canada

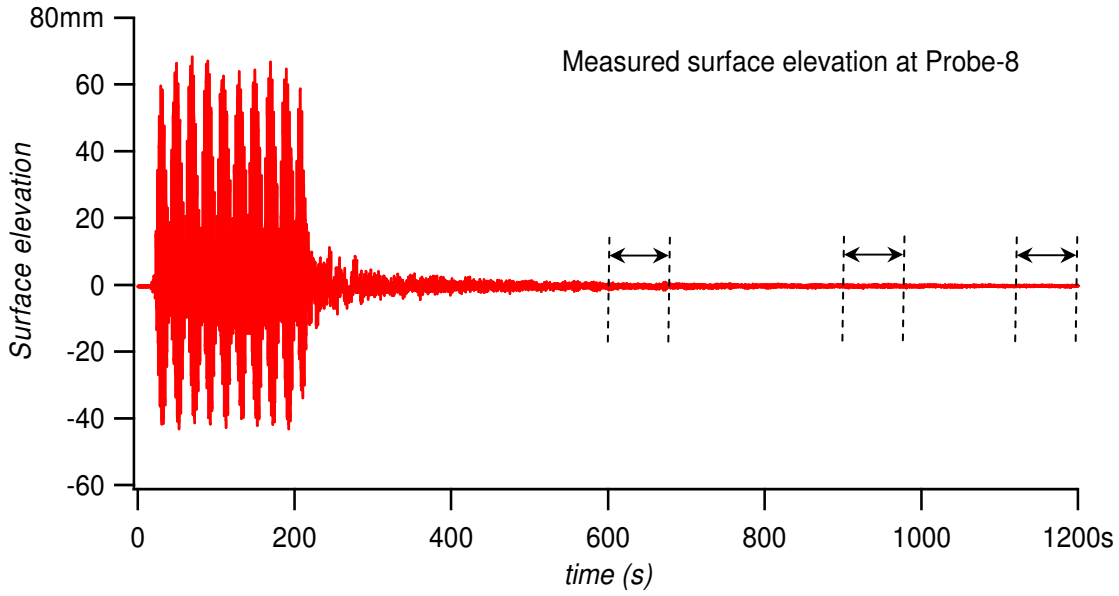

Fig. 7a Measured total surface elevation at P-8 (0 to 20min).
[h=0.4m, H=0.06m, T_1=2.22s and T_2=2.0s]

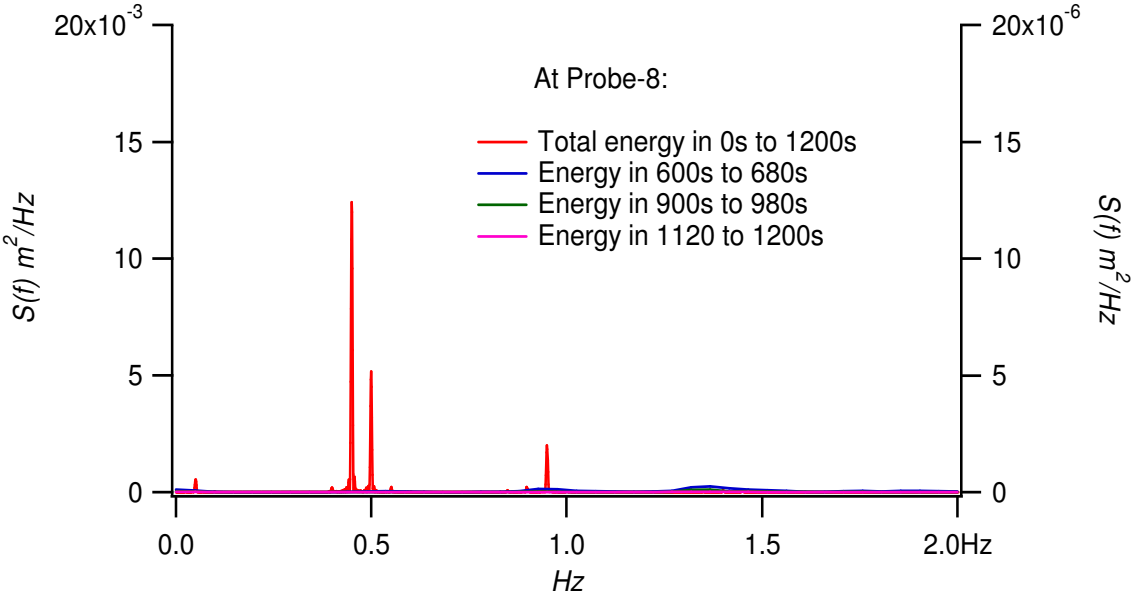

Fig. 7b Total wave energy compared with several segmental energies at P-8.
[h=0.4m, H=0.06m, T_1=2.22s and T_2=2.0s]

 Copyright © 2015 by National Research Council Canada

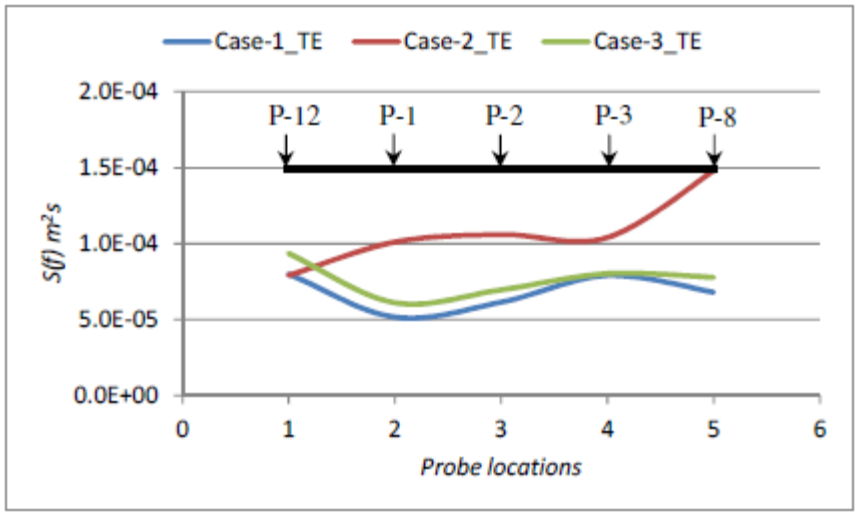

Fig. 8a Comparisons among measured total energy (TE) energies for Case-1, Case-2 and Case-3 at wave probes 12-1-2-3-8.

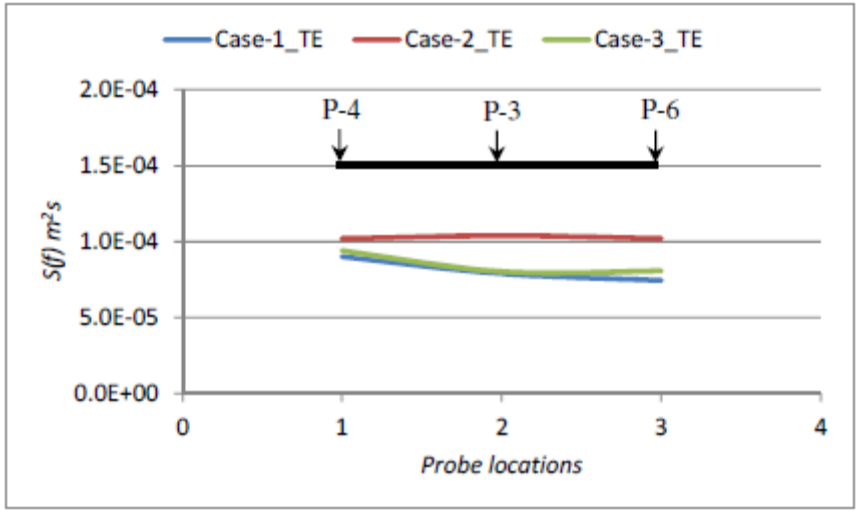

Fig. 8b Comparisons among measured total energy (TE) energies for Case-1, Case-2 and Case-3 at wave probes 4-3-6.

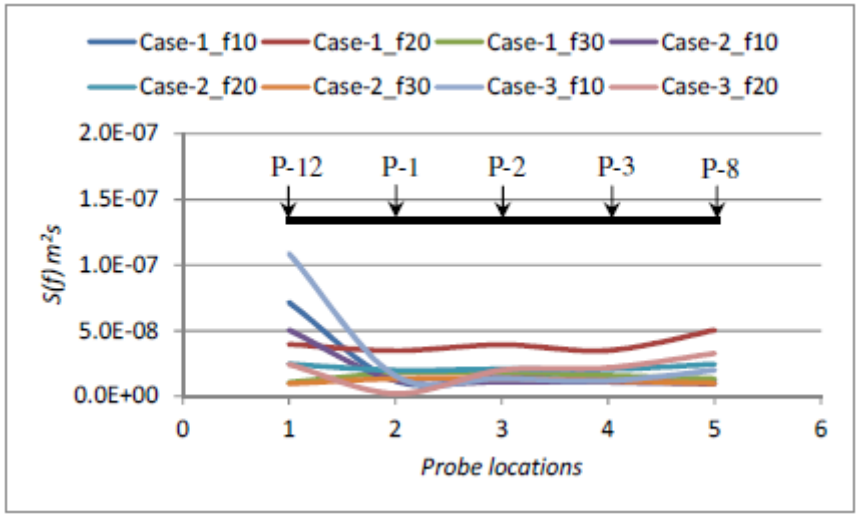

Fig. 8c Comparisons of measured natural frequency energy components (f_{10}, f_{20}, f_{30}) for Case-1, Case-2 and Case-3 at probes 12-1-2-3-8.

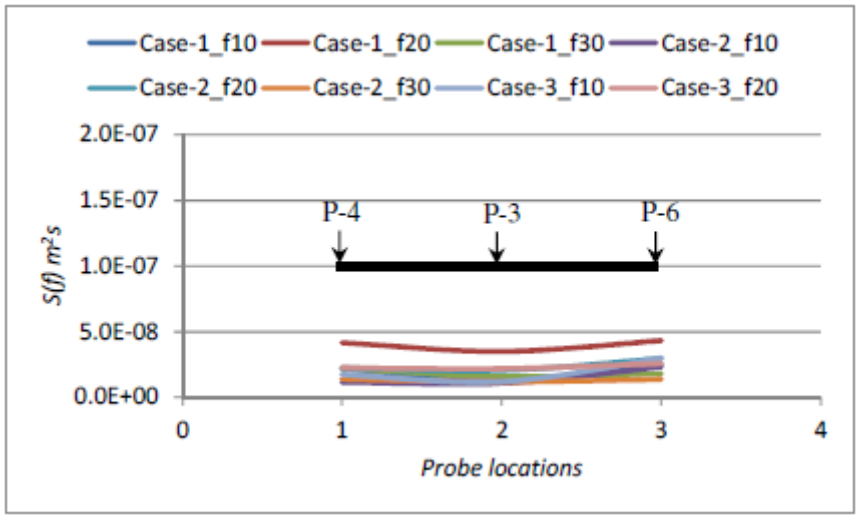

Fig. 8d Comparisons of measured natural frequency energy components for Case-1, Case-2 and Case-3 at probes 4-3-6.

 Copyright © 2015 by National Research Council Canada

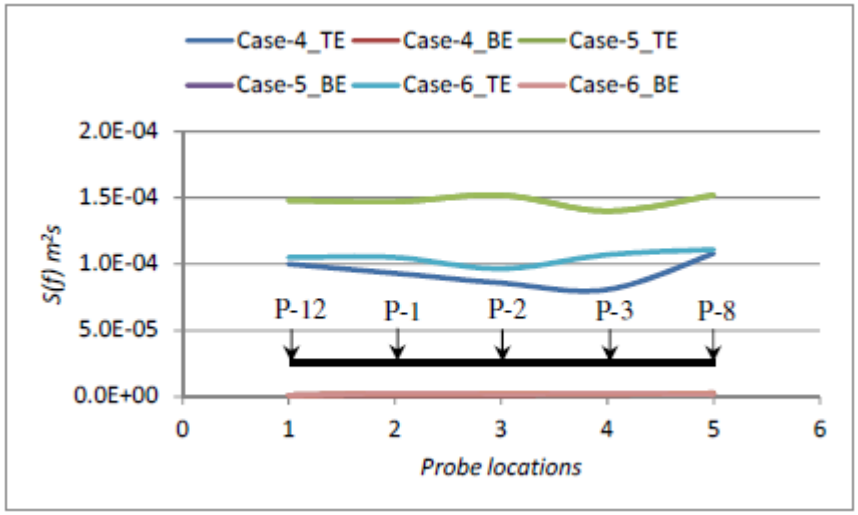

Fig. 9a Measured total (TE) and bounded wave energies (BE) for Case-4, Case-5 and Case-6 at wave probes 12-1-2-3-8.

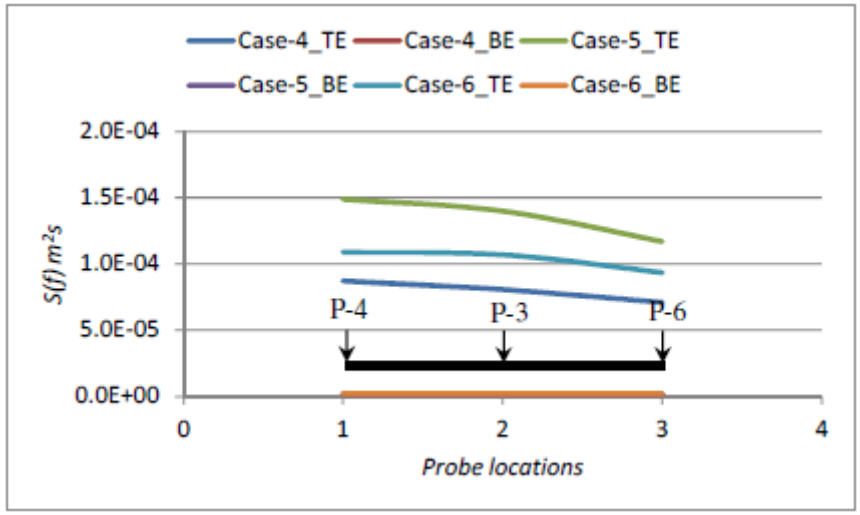

Fig. 9b Measured total (TE) and bounded wave energies (BE) for Case-4, Case-5 and Case-6 at wave probes 4-3-6.

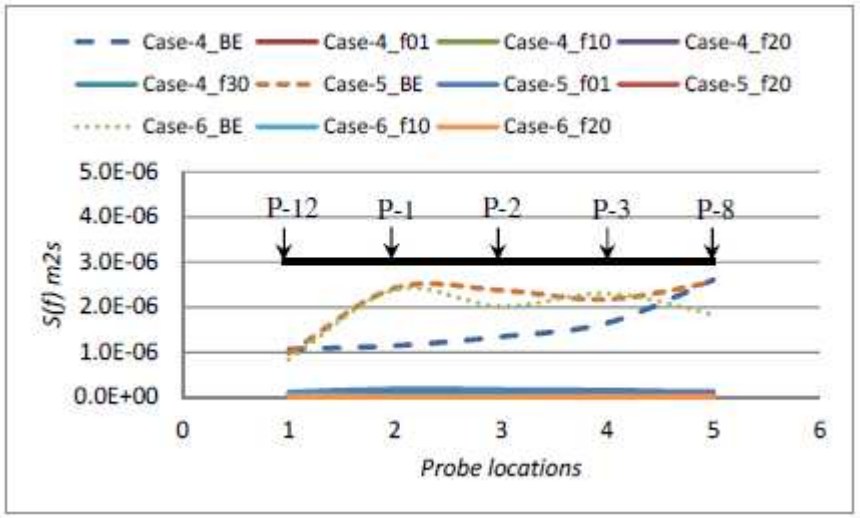

Fig. 9c Measured bounded wave (BE) and natural frequency energy components (f_{01}, f_{10},f_{20},f_{30}) for Case-4, Case-5 and Case-6 at wave probes 12-1-2-3-8.

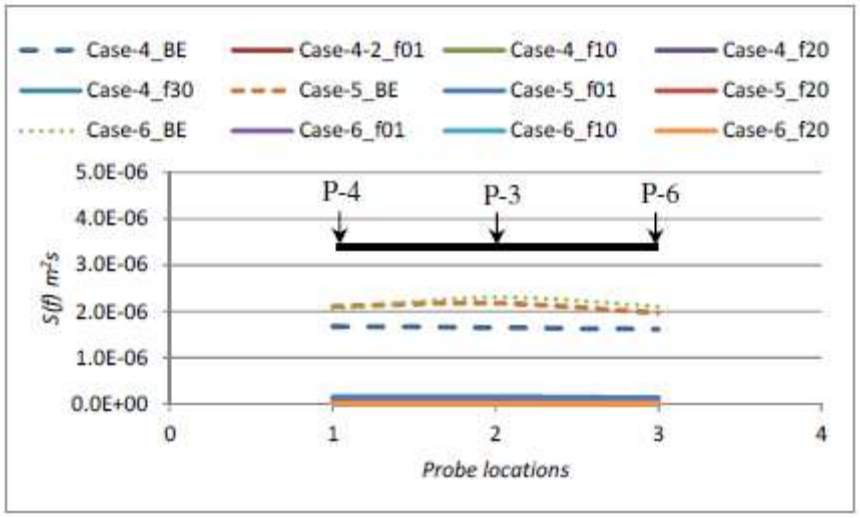

Fig. 9d Measured total (TE) and bounded wave energies (BE) for Case-4, Case-5 and Case-6 at wave probes 4-3-6.

 Copyright © 2015 by National Research Council Canada

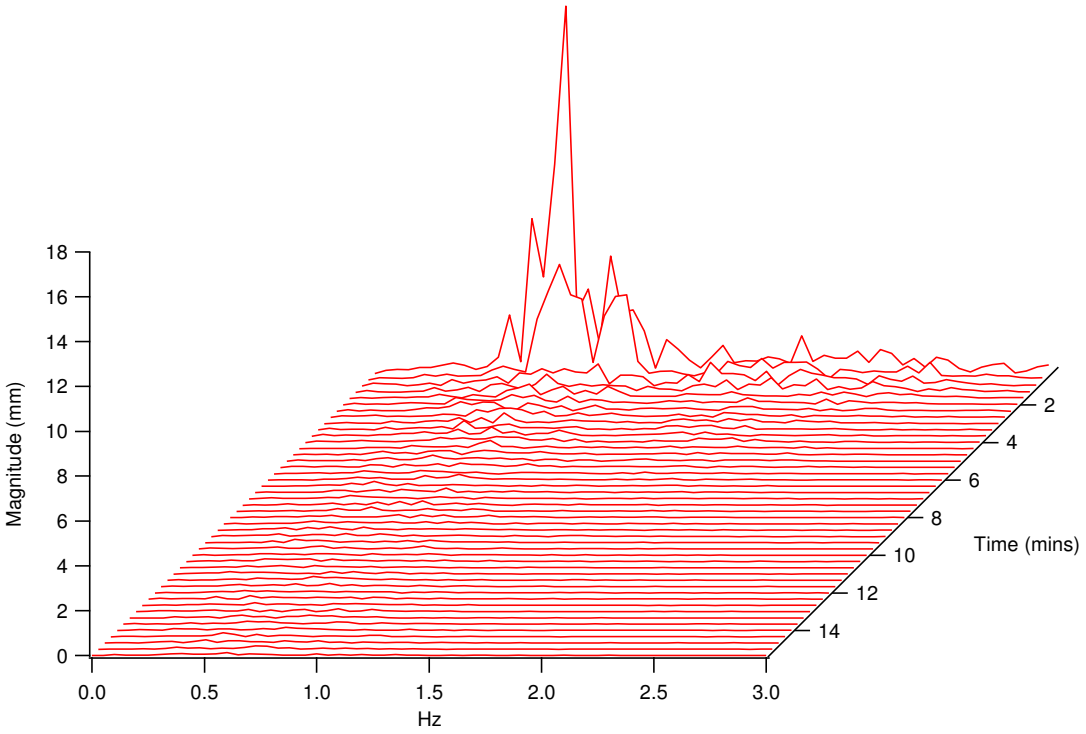

Fig. 10a: Energy spectrum at WP1 for Case-7 when the wave making is terminated
[h=2.28m, H_s = 0.07m and T_p = 1.3s]

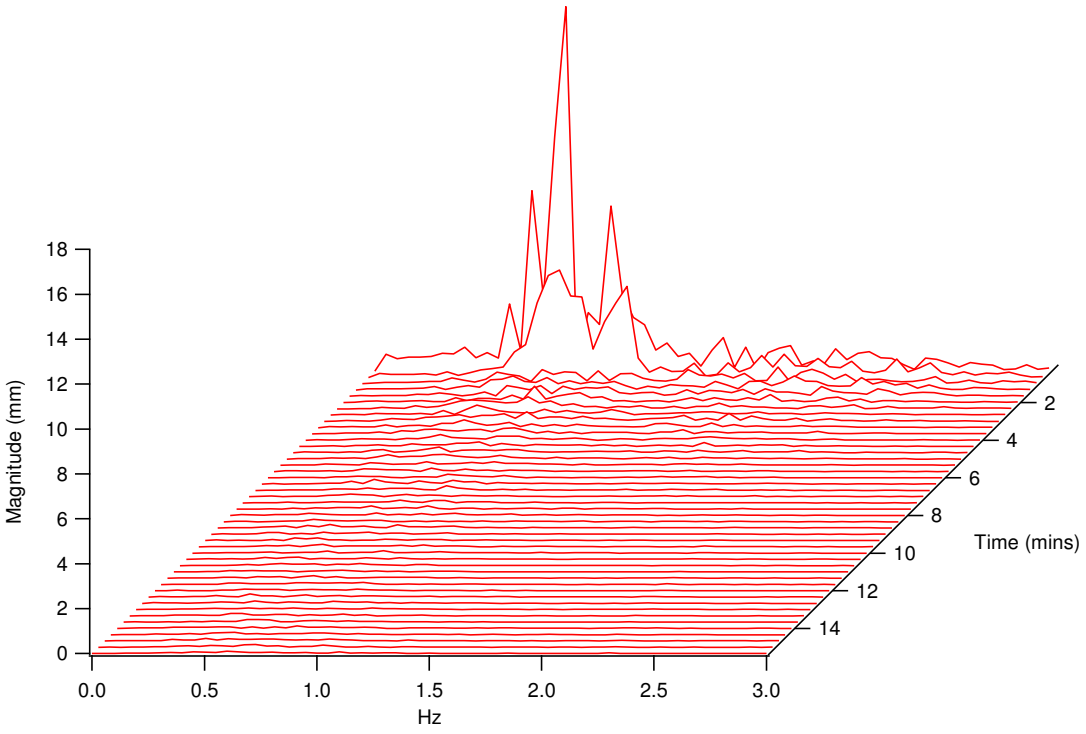

Fig. 10b: Energy spectrum at WP2 for Case-7 when the wave making is terminated
[h=2.28m, H_s = 0.07m and T_p = 1.3s]

 Copyright © 2015 by National Research Council Canada

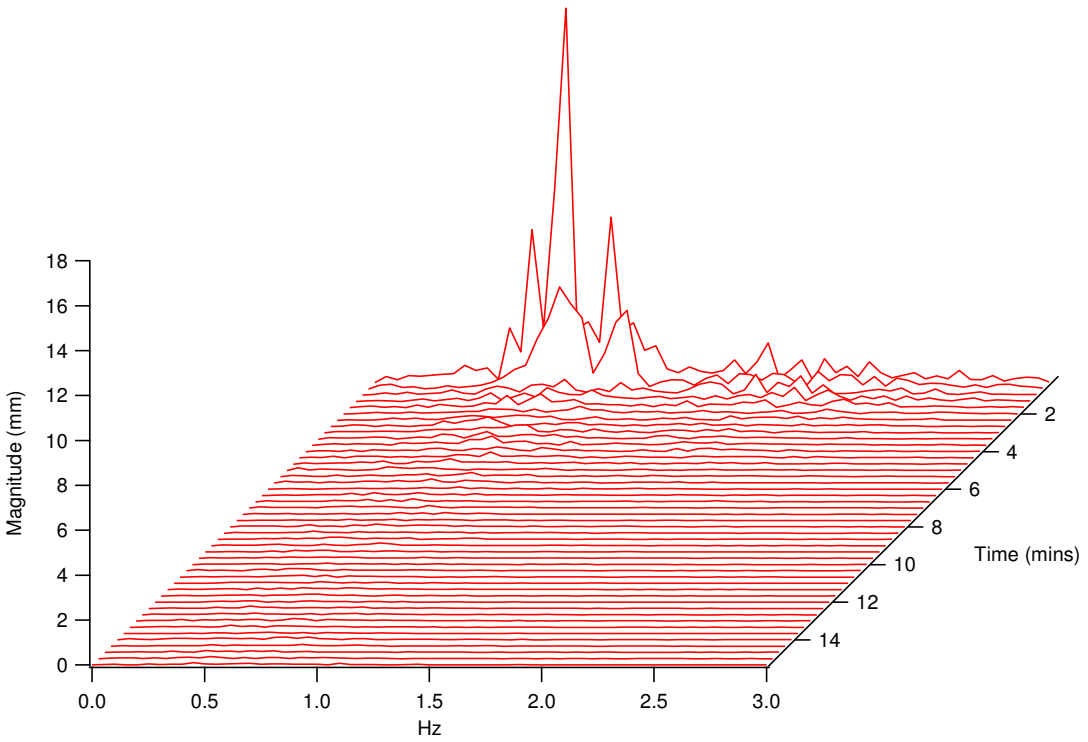

Fig. 10c: Energy spectrum at WP3 for Case-7 when the wave making is terminated
[*h=2.28m, H_s = 0.07m and T_p = 1.3s*]

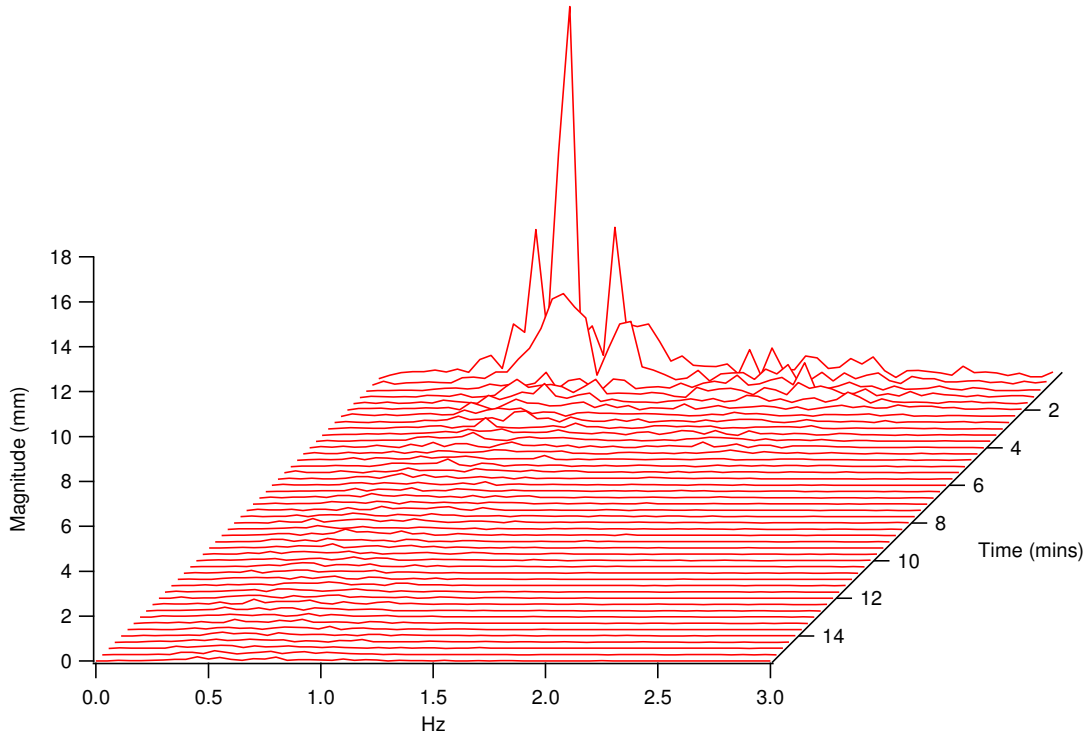

Fig. 10d: Energy spectrum at WP4 for Case-7 when the wave making is terminated
[*h=2.28m, H_s = 0.07m and T_p = 1.3s*]

 Copyright © 2015 by National Research Council Canada

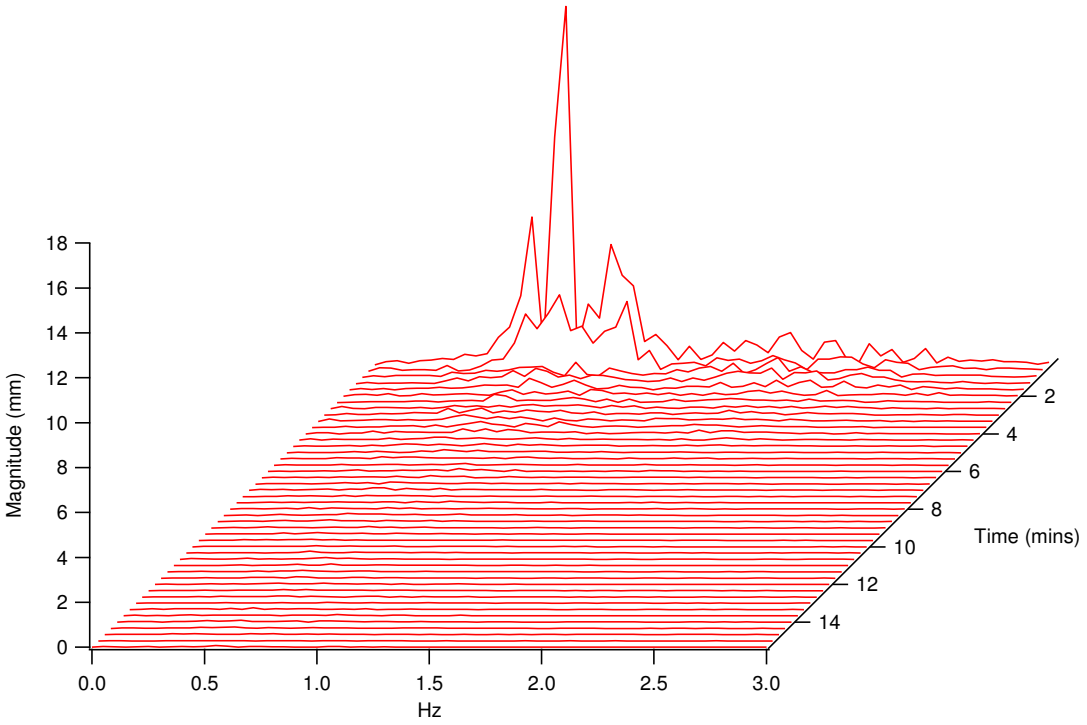

Fig. 10e: Energy spectrum at WP5 for Case-7 when the wave making is terminated
[*h=2.28m,* H_s *= 0.07m and* T_p *= 1.3s*]

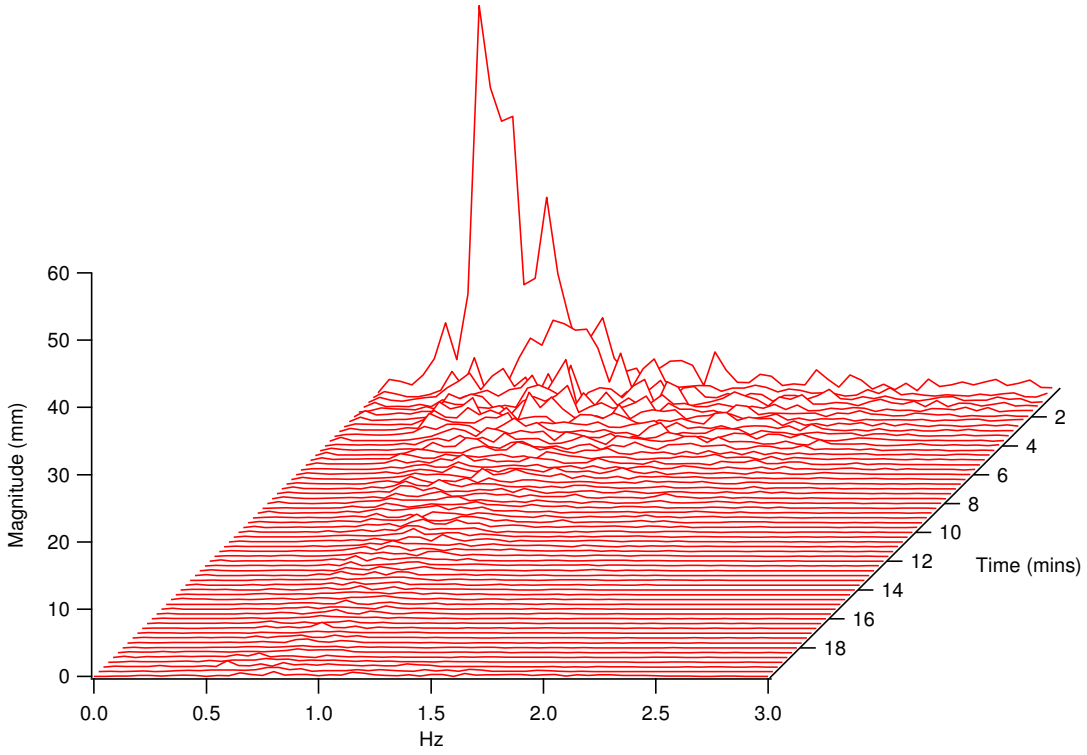

Fig. 11a: Energy spectrum at WP1for Case-8 when the wave making is terminated
[*h=2.28m,* H_s *= 0.39m and* T_p *= 2.6s*]

 Copyright © 2015 by National Research Council Canada

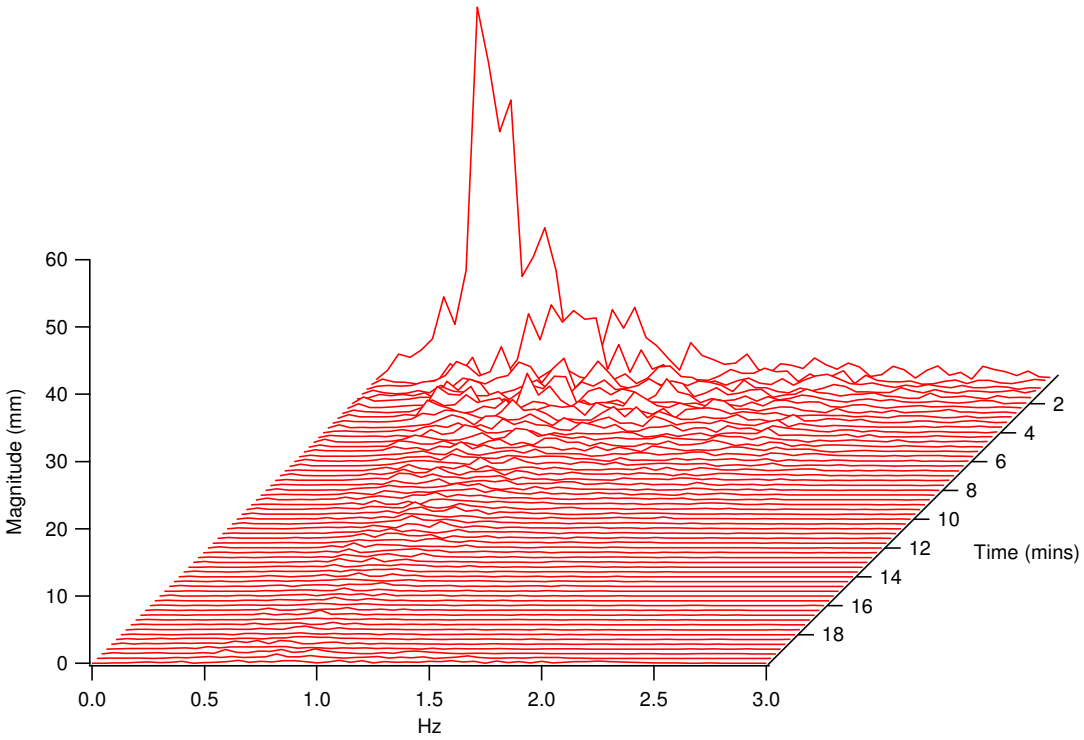

Fig. 11b: Energy spectrum at WP2 for Case-8 when the wave making is terminated
[h=2.28m, H_s = 0.39m and T_p = 2.6s]

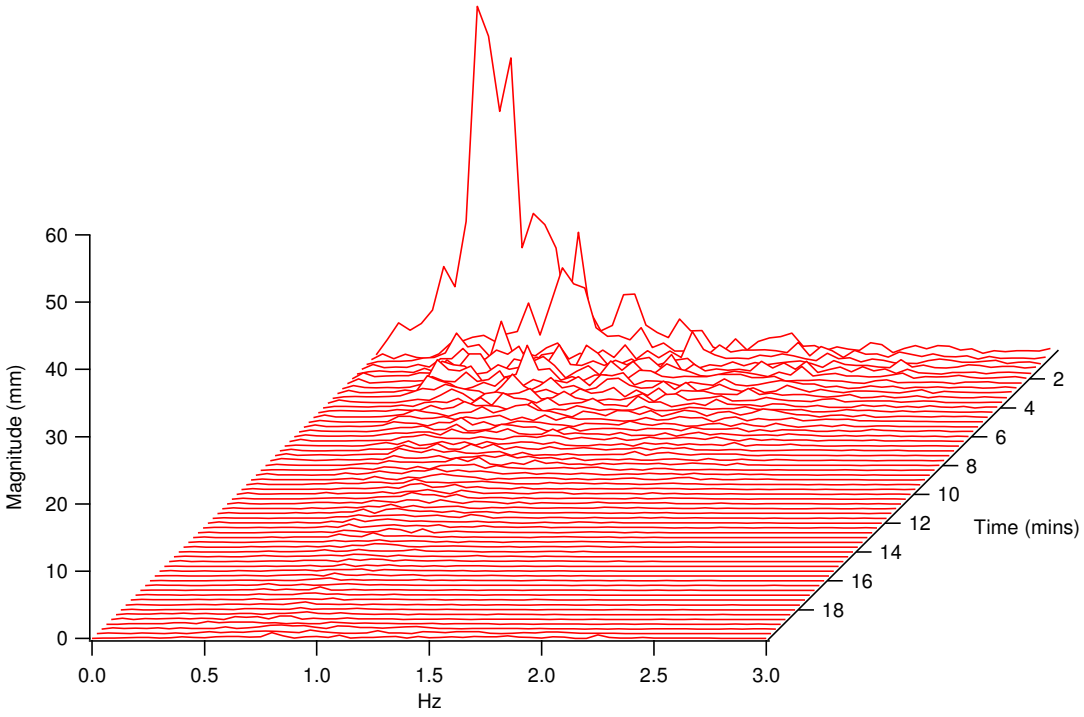

Fig. 11c: Energy spectrum at WP3 for Case-8 when the wave making is terminated
[h=2.28m, H_s = 0.39m and T_p = 2.6s]

 Copyright © 2015 by National Research Council Canada

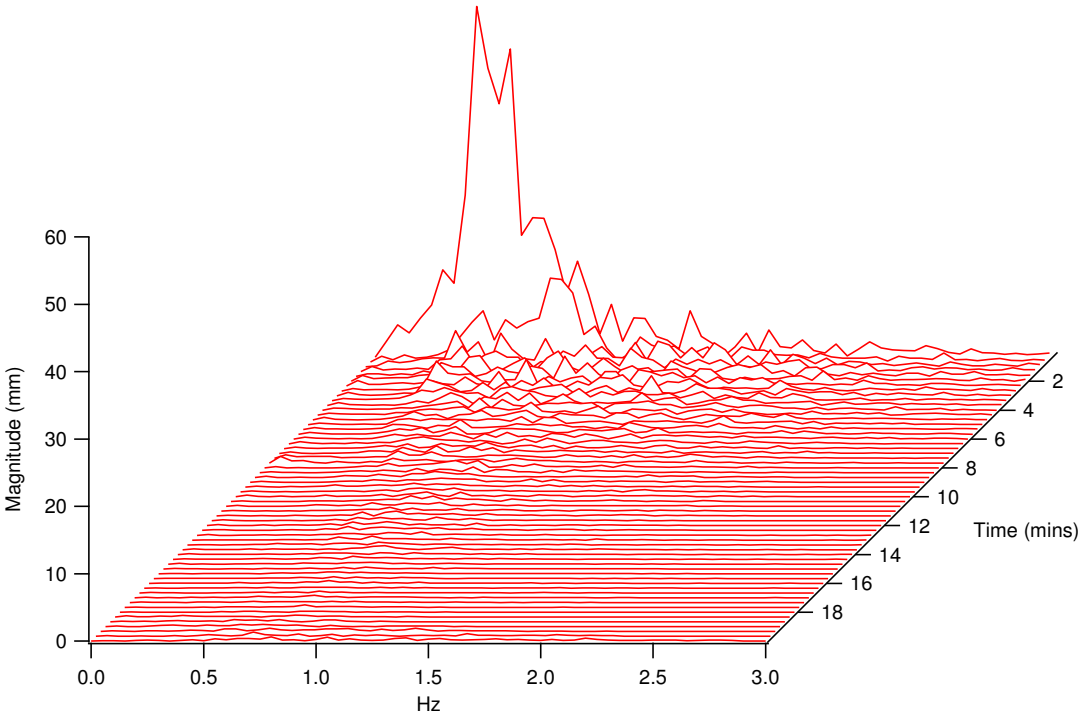

Fig. 11d: Energy spectrum at WP4 for Case-8 when the wave making is terminated
[*h=2.28m, H_s = 0.39m and T_p = 2.6s*]

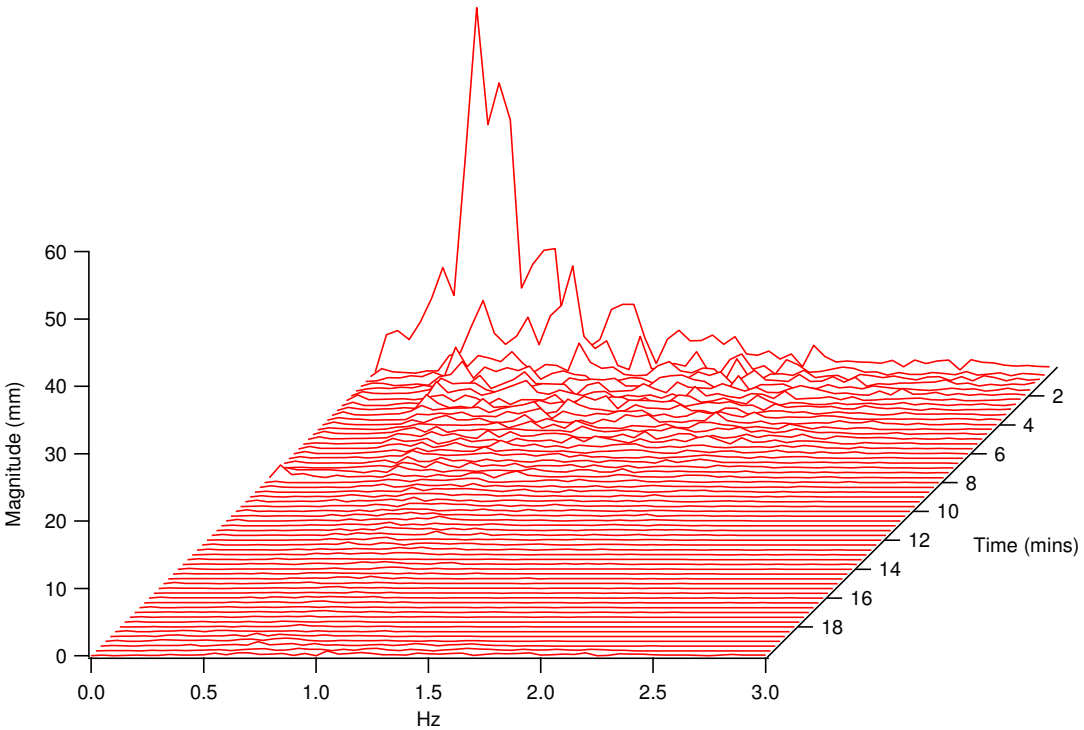

Fig. 11e: Energy spectrum at WP5 for Case-8 when the wave making is terminated
[*h=2.28m, H_s = 0.39m and T_p = 2.6s*]

 Copyright © 2015 by National Research Council Canada